

Effects of ZrO_2 on the properties and dry-pressing preparation of mullite based crossing network structure

Weixia Dong*, Yan Liang, Qifu Bao, Xingyong Gu and Jing-wei Yang

Department of Materials Science and Engineering, Jingdezhen Ceramic Institute, Jingdezhen 333001, P. R. China

Mullite based crossing network structure were dry-pressing prepared by using waste gangue and calmostrin as the main raw material. Effects of ZrO_2 on the properties of the samples were studied. The samples were characterized by X-ray diffraction, scanning electron microscopy and the corresponding energy dispersive analysis. The experiment results showed that when ZrO_2 content was 20%, the sample reached 123.21 MPa of bending strength, 123.75% of bending strength retention rate and the coefficient of thermal expansion of $5.023 \times 10^{-6} / ^\circ C^{-1}$. It could be attributed to the crossing network structure of the mullite, which produced a lot of pore porosity to accommodate a certain expansion deformation and thus alleviate the heat stress. Moreover, micro cracks around the porosity can be formed in the main crack tip region, which decreases local elastic strain energy and restrains the crack propagation and thus enhances the materials properties.

Keywords: Waste gangue, Mullite based crossing network structure, ZrO_2 , drying preparation, Bending strength.

Introduction

Mullite materials have been widely used in metallurgy, chemical industry, petroleum, machinery manufacturing, energy and other industrial areas [1-3]. Its performance improvements play an important role in the comprehensive development, the quality and energy consumption of the products [1]. With the development of ceramics, metallurgy and building materials industries, mullite industries keep a good growth momentum. However, due to the mining, processing and technical level, the comprehensive utilization of resources is not high. Especially, the mineral resources e.g. the high-quality raw material resource are more and more scarce. How to saving and comprehensive utilization of the resources have been an important topic. Therefore, the rational utilization of natural mineral raw materials, such as powder ore, low grade ore, etc have become an important target to realize the sustainable development of mullite industry [2, 3].

Mullite is a kind of typical silicon aluminium silicate, and the typical chemical composition is $3Al_2O_3 \cdot 2SiO_2$. Due to its high melting point, low linear expansion coefficient, high creep activation energy, excellent thermal shock stability and corrosion resistance, etc., mullite has achieved outstanding importance as a material for both traditional and advanced ceramics. However, mullite phase exist very rarely in nature due to its high-temperature and low-pressure conditions. In

recent years, mullite material are prepared by high-temperature solid phase sintering method [3]. However, high temperature sintering makes the mullite grains grow continuously, resulting in a decrease in the mechanical properties and initial properties of the sample. At the same time, when the temperature drops sharply, a large stress occurs between mullite crystals because of the different linear expansion direction of mullite, which causes the destruction of the sintered body. Therefore, the toughening of mullite ceramics is particularly important. Toughened mullite ceramics can improve the performance of single-phase mullite ceramics to a certain extent, thereby improving its bending strength, thermal shock resistance and other properties [4, 5].

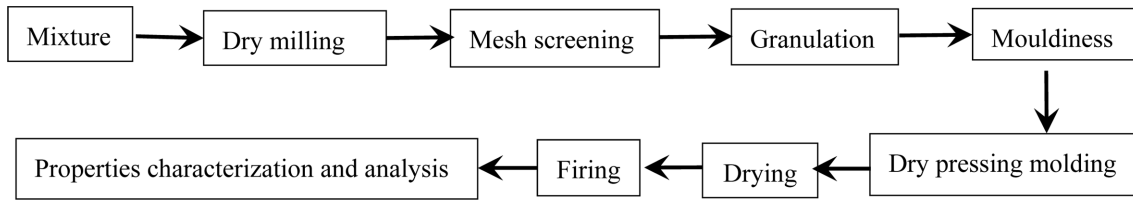
In this paper, mullite based networking structures are dry-pressing prepared by adding zirconium oxide (ZrO_2) using waste gangue as the main raw materials. ZrO_2 exhibit high fracture toughness and bending strength at room temperature [6, 7]. Moreover, ZrO_2 particles react with silicon oxides to form the $ZrSiO_4$ crystals filled in the pore between acicular and long mullite crystals, which is helpful for the bending strength and thermal shock resistance of the samples. Therefore, in order to improve the bending strength and thermal shock resistance of mullite materials, ZrO_2 are introduced in mullite networking structure. Effects of zirconium oxide contents on the properties of mullite based networking structure are discussed.

Experimental Process

Sample preparation

The chemical composition of waste gangue (%):

*Corresponding author:
Tel : +86-571-8480007
Fax: +86-798-8480007
E-mail: weixia_dong@sina.com



Scheme 1. Illustration of the synthesis process.

Al₂O₃ 26.68, SiO₂ 65.21, TiO₂ 1.24, K₂O 3.16, Na₂O 0.43, CaO 0.53, Fe₃O₄ 0.24, IL 16.7. The other chemicals are analytical grade. The mullite precursor composition was prepared by mixing 83.38% waste gangue and 30.54% Al(OH)₃, with the addition of mineralizers (2% V₂O₅ and 3% AlF₃). Batches were prepared by drying mill for 30 min. The grinding material was alumina ball. The sieved powder was to pass 120 mesh and granulated with 6% water, then aged for 24 h. The processed powder was uniaxially pressed under 20 MPa in a steel mold. The samples were put in the oven to dry at 90 °C, followed by placing them on the alumina rollers of an electric furnace to heat at 1,400 °C with a heating rate of 3 °C/min for 1 h. Samples with rectangular shape of 70×10×10 mm were prepared for the bending strength test (Scheme 1).

Characterization

The bending strength of the rectangular-shaped tested samples were characterized by Test Machine (Shenzhen Reger Instrument Co. Ltd. China). The crystal phase of the samples were characterized by X-ray diffraction (XRD, Bruker D8-Advance, German) in a 2θ range from 5° to 70° by using Cu-Kα radiation (λ = 0.15420 nm) operating at 50 kV and 40 mA. The investigation of the microstructures and compositions of the sample powders was done by field emission scanning electron microscopy (FESEM, JSM-6700F, Japan) with an energy dispersive X-ray spectroscopy (EDS) system operating at an accelerating voltage of 5.0 kV or 15.0 kV. Etching solution like hydrofluoric acid solution was used to remove the glassy surface of the fired sample, so that the morphology of the crystal can be revealed. Moreover, RPZ-01 (PANalytical B.V., Holland) was used to analyze the thermal expansion coefficient of the samples. The sintering properties of the fired samples were evaluated based on the Archimedes principle. Thermal shock resistance was characterized by analyzing high bending strength of the samples. The process is as follows: the samples were placed in the furnace heating up to the required temperature of 1,400 °C. After 60 min, the samples are quickly taken from the furnace and then naturally cool in air. After cooling, the high-temperature bending strength of the samples are characterized. The bending strength retention rate of the samples (%) are calculated by means of the following equation [8]:

$$\text{Bending strength retention rate} = \frac{P_0 - P_t}{P_0} \times 100\% \quad (1)$$

P_0 is the bending strength of the fired sample at room temperature, P_t is the bending strength of the sample fired at 1,400 °C for 60 min.

Results and Discussion

Effects of ZrO₂ on the phase of mullite based crossing network structure

Fig. 1 shows XRD patterns of the samples with different ZrO₂ contents. Without the addition of ZrO₂, the pure mullite (JCPDS15–0776) is obtained. With the increase of ZrO₂ contents, the peak intensities of mullite phase at 25.96° decrease, however, those of ZrSiO₄ phase (JCPDS72–0402) and a small amount of m-ZrO₂ (JCPDS 03–0515) increase, indicating ZrSiO₄ phase and a small amount of m-ZrO₂ increase, which is due to the increase of ZrO₂ contents. It can be seen from Al₂O₃-SiO₂ phase diagram [9] that the sample is composed of SiO₂ and mullite solid solution. The formation of ZrSiO₄ is due to the reaction with the abundant SiO₂ and ZrO₂, which will be later discussed in the next section.

Effects of ZrO₂ on the microstructure of mullite based crossing network structure

Fig. 2 shows the SEM images of the sample with the addition of different ZrO₂ contents. Fig. 2(a, b) shows the sample is composed of well-developed mullite

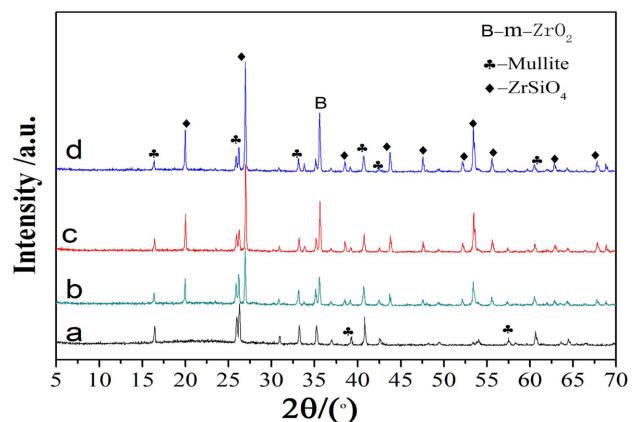


Fig. 1. XRD patterns of the samples with various zirconia contents: (a) 0%, (b) 10%, (c) 20%, (d) 25%.

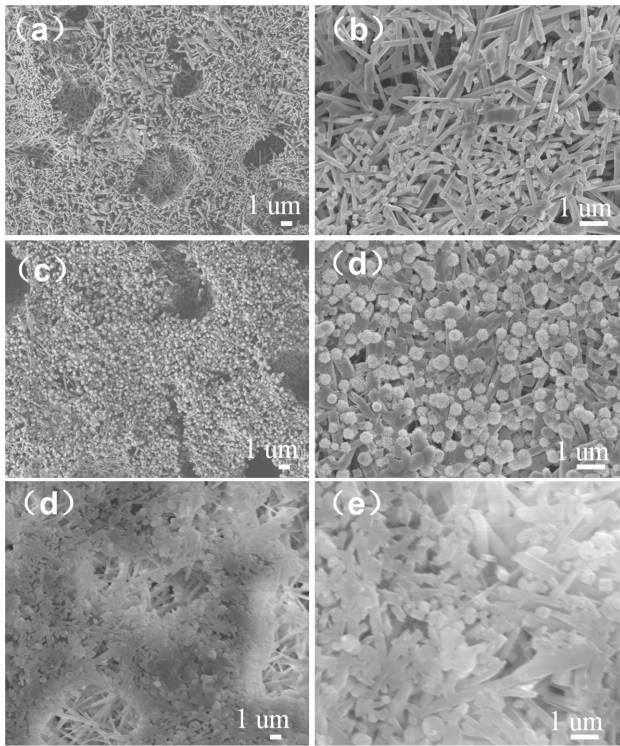


Fig. 2. SEM images of the samples with different zirconia: (a, b) 0%, (c, d) 20%, (e, f) 25%.

Table 1. EDS data of the sample with 20% ZrO₂ for spot A and area B in Fig. 3.

Elements	Spot A		Area B	
	Weight percent	Atomic percent	Weight percent	Atomic percent
F K	4.93	5.33	6.71	7.23
Al K	-	-	32.75	24.84
Zr K	32.29	35.39	-	-
Si K	9.88	35.29	12.39	9.03
Ca K	0.56	0.29	0.56	0.29
Ti K	0.59	0.25	0.80	0.34
V K	0.45	0.23	1.00	0.40
Fe K	0.63	0.14	0.76	0.28
O K	49.97	59.82	45.03	57.58
Total	100.00		100.00	

columnar with crossing network structure, which provides an enough interspace for the growth of mullite without the addition of ZrO₂. When ZrO₂ content is 20%, the sample exhibits well-developed mullite columnar structure (Fig. 2(c)). From the enlarged SEM image (Fig. 2(d)), many uniform particles fill in the pores due to the formation of the mullite crossing network. Increasing ZrO₂ content to 25%, the mullite columnar is poor, and the uniform particles increase and cluster together, the sample is dense which is harmful for the growth of mullite (Fig. 2(e, f)). And there are some isolated spherical pores existing in the fractured surface of the samples, which indicate the existence of the

liquid phase and the viscous flow mechanism [8]. The existence of viscous flow can also be verified from the EDS analysis (Table 1) and SEM images (Fig. 3).

Fig. 3 EDS spectrum of the sample with the addition of 20% ZrO₂. It can be seen that the columnar particles contain Ca, Fe, F, V, Ti, Al, Si and O elements, Zr elements are not detected. However, small particles are only composed of Ca, Fe, F, Zr, V, Ti, Si and O elements. Combining with XRD and EDS results, it could be concluded that columnar particle maybe be mullite phase [6], and small particles maybe be ZrSiO₄ and m-ZrO₂ phase. To further confirm the composition with different shape particles, element quantitative analysis for A and B spots are analyzed as shown in Table 1. The corresponding EDS spectrum shown in Table 1 reveal that the spot A for columnar particle consist of Al and Si contents with an atomic ratio of about 3:2, which are close to the stoichiometry of mullite, and the spot B for small particles consist of Zr and Si contents with an atomic ratio of about 1:1, which are close to the stoichiometry of ZrSiO₄. The glass around the mullite crystals and ZrSiO₄ contains elements of Ca, Fe, F, V, Ti, indicating the glass phase forms from a liquid containing impurities at firing temperature, which may be from the composition of waste gangue, V₂O₅ and AlF₃. The liquid phase significantly increases by extensive incorporation of liquid during firing at 1,400 °C, while the viscosity of liquid phase favors the growth of mullite crystals and promotes the formation of ZrSiO₄ particles due to the reaction with ZrO₂ and SiO₂ (Fig. 1) via viscous flow mechanism, which is similar with our previous report [8]. Thus a positive effect on the bending strength of the sample is exerted, conversely, In addition, the interlocking texture constructed by mullite crystals also favors the bending strength of the samples.

Effects of ZrO₂ on the porosity and bending strength of mullite based crossing network structure

Fig. 4 shows the porosity curves of the samples with different ZrO₂ contents. It can be obviously seen that the porosity of the sample increases with the increase of ZrO₂ contents, and when ZrO₂ contents are more than 15%, the increase in the porosity of the sample becomes slowly. Zirconia toughening is used to monoclinic phase into a tetragonal zirconia inducing microcrack toughening, which is one of the three kinds of toughening mechanisms. After adding zirconia, zirconium oxide would transform from the monoclinic zirconia to tetragonal zirconia at 1,170 °C with around 7% of the volume change during the transformation and thus makes the samples produce many tiny micro cracks, which toughen the properties of the material [11, 12]. At the same time, the binary or multiple liquid produced from the reaction among the impurity e.g., CaO, TiO₂ and Fe₂O₃ of waste gangue, AlF₃, V₂O₅, Al₂O₃ and SiO₂ [13, 14], which is helpful for the growth of the network structure constructed by

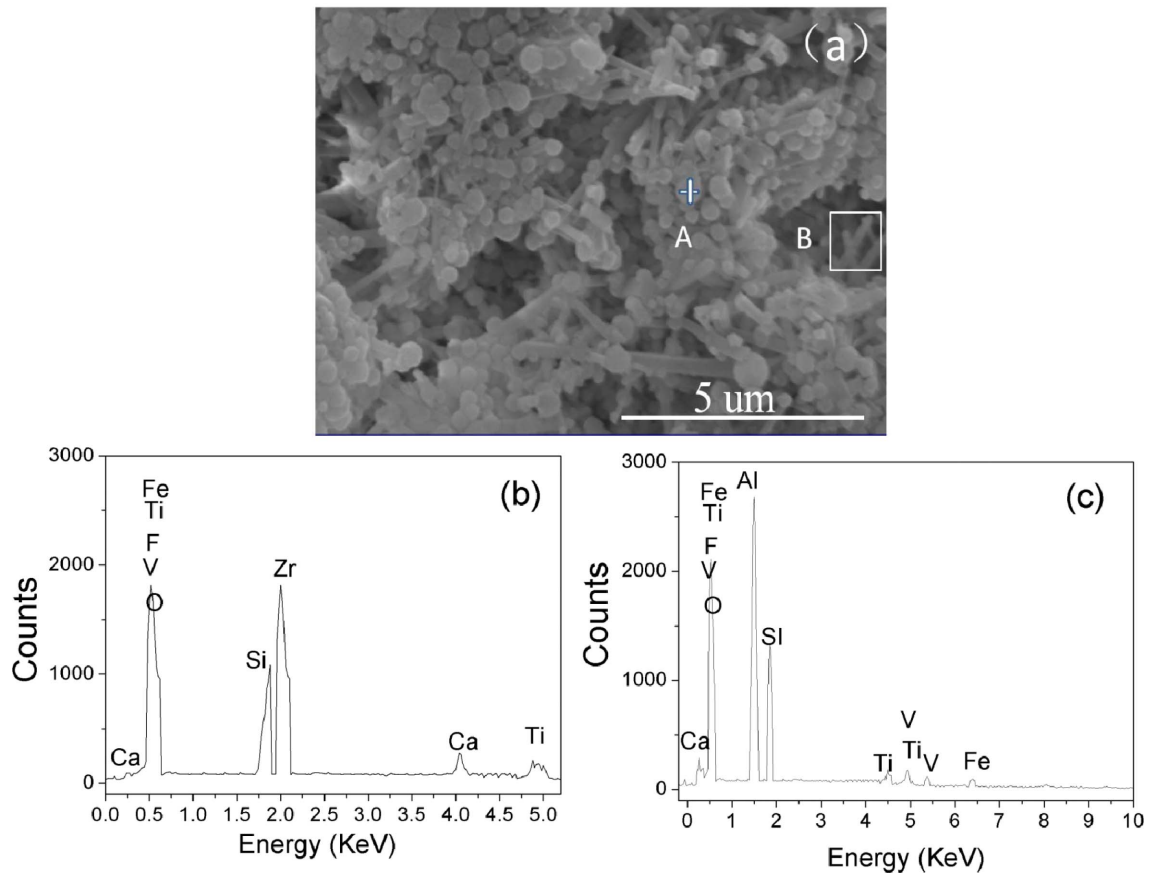


Fig. 3. EDS spectra of the sample with 20% ZrO_2 : (b) Spot A in Fig. 3(a), (c) Area B in Fig. 3(a).

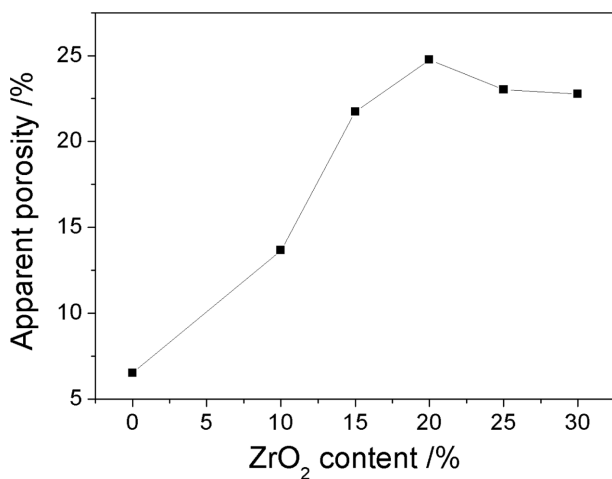


Fig. 4. Apparent porosity curves of the samples with different zirconium oxide.

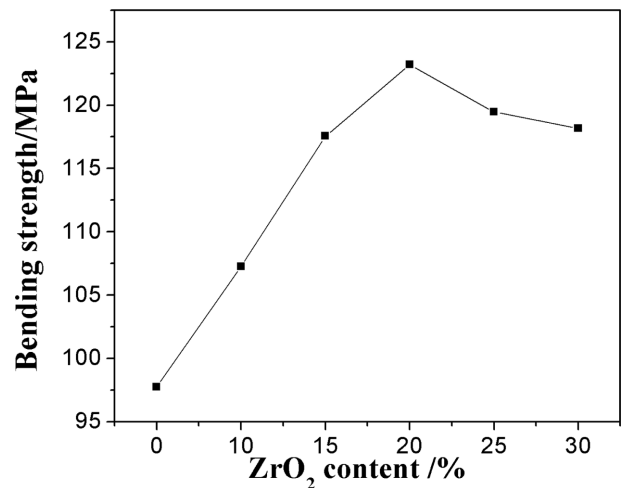


Fig. 5. Bending strength curves of the samples with different zirconium oxide.

long and acicular mullite crystals (Fig. 2). So the porosity of the samples increased gradually. Further increasing zirconia contents to 25%, zircon phases increase (Fig. 1(d)), then grow up and gather themselves together, and thus prevent the growth of the mullite. Therefore mullite columnar crystal is short and the network structure of mullite decreases (Fig. 2(e, f)), and thus the densification degree of the sample increases, which are

consistent with XRD and SEM results, so the porosity of the sample decreases.

Fig. 5 shows the bending strength of the sample with the various ZrO_2 content. The bending strength of the samples increases with the increase of ZrO_2 contents firstly and then decreases. It is surprising that the sample prepared by adding 20% ZrO_2 has the maximum value of 123.21 MPa, although the porosity of the sample by

adding 20% ZrO₂ is higher than that of the others (Fig. 4). ZrO₂ content affects the bending strength of the samples by controlling the growth of network structure constructed by mullite crystals, crystallinity, the micro cracks based on the phase transition of zirconia, and porosity of the samples. It is known that the transformation of zirconia reduces some micro cracks formation, which consumes its elastic energy consumption and thus improves the bending strength of the samples [17]. For the growth of network structure constructed by mullite crystals, with the increase of ZrO₂ content (Fig. 2), well-developed mullite columnar with crossing network structure become poor and the mullite crystals decrease, the defects of the crystal increase, thus the bending strength of the samples decreases. As ZrSiO₄ phase and m-ZrO₂ crystallinity increase keeping the mullite almost unchanged, more ZrSiO₄ crystals filled in the interspace of the mullite networking, and the transformation of zirconia, which improved the bending strength of the samples [17]. On the other hand, as for the porosity, it is common that the fracture surface energy of the samples tends to decrease with the increase of the porosity and the pore exists as a defection, so the samples with the smaller porosity have the larger bending strength. However, it is worth pointing out that in the presence of the high stress gradient due to the zirconia transformation in the present experiment, the pore between the mullite networking could accommodate the deformation and prevent crack propagation, which improves the bending strength of the samples [16]. Accordingly, when ZrO₂ content is $\leq 20\%$, the increase of bending strength can be ascribed to the enhancement of the ZrSiO₄ phase and m-ZrO₂ crystallinity, well-developed mullite columnar with crossing network structure and increase of porosity with increasing ZrO₂ content (Fig. 2, Fig. 3 and Fig. 4). However, when ZrO₂ is more than 25%, the ZrSiO₄ crystallinity and porosity decrease dramatically (Fig. 1(d) and Fig. 4), lots of ZrSiO₄ particles incline to aggregate itself and grow into continuous beaded structure, which would destroy the mullite network (Fig. 2(e, f)) and decrease the porosity of the sample, so the bending strength of the sample decreases.

Fig. 6 shows the bending retention analysis diagram of the sample with the various addition of ZrO₂. Table 2 shows the thermal expansion coefficient (40~800°C) of the samples with the addition of 20% ZrO₂ and without ZrO₂. It can be seen that from Fig. 6 and Table 2, with the increase of ZrO₂ contents ($\leq 20\%$) obviously enhanced the thermal shock resistance of the samples and lower the thermal expansion due to the micro cracks based on the phase transition of zirconia, the increased zircon content and porosity of the samples (Fig. 5). When ZrO₂ contents is 20%, the bending retention strength of the sample is 123.75% and the coefficient of thermal expansion decrease. It is well known that thermal expansion coefficient of zircon,

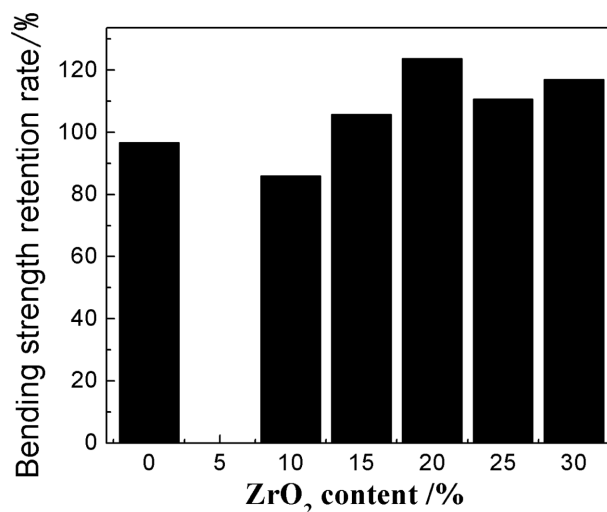


Fig. 6. Bending strength retention rate curves of the samples with different zirconium oxide.

Table 2. Thermal expansion coefficient of the samples doped with zirconium oxide.

Mass fraction of ZrO ₂ /%	Thermal expansion coefficient ($\times 10^{-6} \text{ } ^\circ\text{C}^{-1}$) (40~800 °C)
0	5.038
15	5.026
20	5.023
25	5.896

zirconia and mullite is $4.51 \times 10^6 \text{ } ^\circ\text{C}^{-1}$, $10.3 \times 10^6 \text{ } ^\circ\text{C}^{-1}$ and $5.32 \times 10^6 \text{ } ^\circ\text{C}^{-1}$, respectively [18]. After adding ZrO₂, from the result of XRD, it is obvious that zircon is produced which is higher than m-ZrO₂ content (Fig. 1). Although the thermal expansion coefficient of zirconia is large, based on experimental result (Table 2), it indicates that when ZrO₂ contents is suitable ($\leq 20\%$), the micro cracks due to the phase transition of zirconia, the increased zircon content and porosity of the samples are dominated as main factors for lowering the thermal expansion coefficient in our experiment. Therefore, the thermal expansion coefficient of the samples is lowered. When the thermal expansion coefficient of the sample is smaller, the volume change of materials caused by temperature is smaller and thus the corresponding temperature stress is smaller and thermal shock resistance is better, therefore, the bending retention of the sample is more than that of the sample without ZrO₂. At the same time, it maybe attribute to microcracks originated in the changes in the volume of the transformation of zirconia crystal, and mullite with the well-perfect interlaced network structure produced a lot of porosity which could accommodate a certain expansion deformation and thus reduce the thermal stress. In common, porosity is found in other intergranular and micro cracks are slightly more originated on the grain boundary or near other microstructure defects, hence

porosity can form local network in the main crack tip region, which decreases local elastic strain energy and restrains the crack propagation, thus improves the material bending retention [9-14]. However, further increasing ZrO₂ content, due to decreased porosity and poor mullite interlaced network structure of the samples, the large thermal expansion coefficient of zirconia is dominated as main factors, Thus, the thermal expansion of the samples increases.

Conclusions

Mullite based networking structure was dry-pressing prepared by adding ZrO₂ using waste gangue and aluminium hydroxide as the main raw material. XRD pattern shows that with the increase of amount of ZrO₂, mullite phases decrease, however, zircon and m-ZrO₂ increase. The porosity, bending strength and the retention bending strength of the samples firstly increase and then decrease, and the thermal expansion coefficient decreases. When the zirconia content is 20%, the bending strength of 123.21 MPa, retention bending strength of 123.75%, thermal expansion coefficient of $5.023 \times 10^{-6}/^{\circ}\text{C}^{-1}$ of the sample obtain the optimum values. It indicated that moderate ZrO₂ content could improve the performance of the mullite based material. SEM images exhibited that appropriate amount of ZrO₂ (20%) was conducive to form ZrSiO₄ particles filling into gaps in a network structure, and thus enhanced toughening effect. It will be a good application prospect as a refractory material.

Acknowledgement

The present work was supported by Educational Major Project of Jiangxi Province in China (GJJ190707 and GJJ201301).

References

1. M. Zhao and J. Liang, *J. Gra. Natur. Sci. Med.* 33 (2012) 17-19.
2. D. Xu and S. Wang, *Chn. Steel.* 5 (2011) 11-15.
3. H. Schneider, J. Schreuer, and B. Hildmann, *J. Eur. Ceram. Soc.* 28[2] (2008) 329-344.
4. K. Cui, Y. Zhang, T. Fu, J. Wang, and X. Zhang, *Coatings.* 10[7] (2020) 672.
5. C. Sadik, I. Amrani, and A. Albizane, *J. As. Ceram. Soc.* 2[2] (2014) 83-96.
6. M. Hamidouche, N. Bouaouadja, H. Osmani, R. Torrecillas, and G. Fantozzi, *J. Eur. Ceram. Soc.* 16[4] (1996) 441-445.
7. J. Guo and P. Zhu, *J. CHN. Ceram. Soc.* 1 (1996) 7-17.
8. X. Gu, P. Li, W. Dong, and T. Luo, *Key. Eng. Mater.* 602-603 (2014) 628-631.
9. G. Li and C. Zhang, in "Phase basement and refractory material diagrams" (Metallurgical Industry Press, 1994) p.1.
10. W. Dong, Q. Bao, X. Gu, H. Shen, and J. Yang, *J. Ceram. Soc. Jpn.* 125[2] (2017) 75-78.
11. N.M. Rendtorff, L.B. Garrido, and E.F. Aglietti, *Ceram. Int.* 34[8] (2008) 2017-2024.
12. N.M. Rendtorff, L.B. Garrido, and E.F. Aglietti, *Ceram. Int.* 35[2] (2009) 779-786.
13. A. Gungor, O. Celikcioglu, and S. Sahin, *Ceram. Int.* 38[5] (2012) 4189-4194.
14. T.M. Souza, A.P. Luz, M.A.M. Brito, and V.C. Pandolfelli, *Ceram. Int.* 40[1] (2014) 1699-1707.
15. N.M. Rendtorff, L.B. Garrido, and E.F. Aglietti, *Mat. Sci. Eng. A* 498[1-2] (2008) 208-215.
16. S. Xia and X. Zhu, *Refract.* 4 (1998) 192-194.
17. G.T.M. Stam, E.V.D. Giessen, and P. Meijers, *Int. J. Sol. Struct.* 31[14] (1994) 1923-1948.
18. I. Yu. Prokhorov, G.Y. Akimov, and V.M. Timchenko, *Refract. Ind. Ceram.* 39[5] (1998) 189-197.